Recovery of Photoinduced Reversible Dark States Utilized for Molecular Diffusion Measurements

ARTICLE *in* ANALYTICAL CHEMISTRY · DECEMBER 2010

Impact Factor: 5.64 · DOI: 10.1021/ac1014047 · Source: PubMed

3 AUTHORS:

Andriy Chmyrov
Helmholtz Zentrum München
12 PUBLICATIONS **287** CITATIONS

SEE PROFILE

Tor Sandén
KTH Royal Institute of Technology
19 PUBLICATIONS **211** CITATIONS

SEE PROFILE

Jerker Widengren
KTH Royal Institute of Technology
108 PUBLICATIONS **3,966** CITATIONS

SEE PROFILE

Anal. Chem. **2010,** *82,* 9998–10005

Recovery of Photoinduced Reversible Dark States Utilized for Molecular Diffusion Measurements

Andriy Chmyrov, Tor Sandén, and Jerker Widengren*

Experimental Biomolecular Physics, Department of Applied Physics, Royal Institute of Technology, SE-10691 Stockholm, Sweden

For a spatially restricted excitation volume, the effective modulation of the excitation in time is influenced by the passage times of the molecules through the excitation volume. By applying an additional time-modulated excitation, the buildup of photoinduced reversible dark states in fluorescent molecules can be made to vary significantly with their passage times through the excitation volume. The variations in the dark state populations are reflected by the time-averaged fluorescence intensity, which thus can be used to characterize the mobilities of the molecules. The concept was experimentally verified by measuring the fluorescence response of freely diffusing cyanine fluorophores (Cy5), undergoing trans−cis isomerization when subject to time-modulated excitation in a focused laser beam. From the fluorescence response, and by applying a simple photodynamic model, the transition times of the Cy5 molecules could be well reproduced when applying different laminar flow speeds through the detection volume. The presented approach puts no constraints on sample concentration, no requirements for high time resolution or sensitivity in the detection, nor requires a high fluorescence brightness of the characterized molecules. This can make the concept useful for a broad range of biomolecular mobility studies.

Fluorescence offers several means to measure translational diffusion of biomolecules in cells, cellular membranes, lipid bilayers, and in solutions. Fluorescence recovery after photobleaching (FRAP) and fluorescence correlation spectroscopy (FCS) are together with single-particle tracking (SPT) probably the most widely used techniques.[1] The FCS and FRAP techniques date back to the 1970s[2−5] but have experienced an increased interest for diffusion studies in the last decades, in particular for cellular measurements.[6] In FCS, diffusion properties of fluorescent molecules are analyzed via the fluorescence intensity fluctuations as the molecules transit a confocal detection volume. In FRAP, the fluorescent molecules in a defined volume are bleached by a laser pulse, and the subsequent fluorescence intensity recovery as unbleached fluorescent molecules diffuse into the bleached region provides the molecular mobility information. FCS and FRAP are complementary in the sense that they cover different concentration ranges, spatial resolutions, and time regions.[7] As a molecular fluctuation technique FCS is typically limited to concentrations of fluorescent molecules below 500 μm^{-2} in membranes and 500 nM in solutions. FRAP cannot be applied at as low concentrations as FCS (or SPT) but works well at concentrations far higher than the upper limits of the FCS technique. Spatially, FRAP integrates the diffusive properties of the molecules over a much larger region than by FCS, which monitors the diffusive properties of the molecules only when in the detection volume itself. Temporally, FCS can monitor molecular movements down to microseconds, while FRAP is better suited to slower processes in the time range up to seconds. Both FCS and FRAP put restrictions on the fluorophore labels. In FCS, they should be photostable and able to yield high fluorescence emission rates.[8] In FRAP, the fluorophores should be moderately sensitive to photobleaching to minimize the intensity and duration of the bleach beam, but not so sensitive that significant bleaching occurs when measuring the fluorescence recovery by the attenuated probe beam.[9] Moreover, the photobleaching process itself needs to be defined. In particular, reversible photobleaching, i.e., any spontaneous recovery of fluorescence not attributed to diffusion, is a concern and may lead to serious misinterpretations of the diffusion behavior of the studied molecules.[9]

In this work we propose the exploitation of reversible photobleaching for diffusion measurements. By FCS, transitions of dye molecules to and from photoinduced, long-lived, dark, or weakly emitting states can be well characterized via the related fluorescence fluctuations.[10−14] However, information about these states can also be extracted from the variation in the time-averaged fluorescence of dye molecules under different regimes of time-

* To whom correspondence should be addressed. E-mail: jerker@biomolphysics.kth.se. Phone: +46-8-55378030.

(1) Day, C. A.; Kenworthy, A. K. *Biochim. Biophys. Acta* **2009**, *1788*, 245–253.
(2) Magde, D.; Elson, E.; Webb, W. W. *Phys. Rev. Lett.* **1972**, *29*, 705–708.
(3) Elson, E. L.; Magde, D. *Biopolymers* **1974**, *13*, 1–27.
(4) Axelrod, D.; Koppel, D. E.; Schlessinger, J.; Elson, E.; Webb, W. W. *Biophys. J.* **1976**, *16*, 1055–1069.
(5) Koppel, D. E.; Axelrod, D.; Schlessinger, J.; Elson, E. L.; Webb, W. W. *Biophys. J.* **1976**, *16*, 1315–1329.
(6) Sprague, B. L.; McNally, J. G. *Trends Cell Biol.* **2005**, *15*, 84–91.
(7) Guo, L.; Har, J. Y.; Sankaran, J.; Hong, Y.; Kannan, B.; Wohland, T. *ChemPhysChem* **2008**, *9*, 721–728.
(8) Koppel, D. E. *Phys. Rev. A* **1974**, *10*, 1938–1945.
(9) Verkman, A. S. In *Methods in Enzymology*; Gerard, M., Ian, P., Eds.; Academic Press: San Diego, CA, 2003; Vol. 360, pp 635−648.
(10) Widengren, J.; Mets, Ü.; Rigler, R. *J. Phys. Chem.* **1995**, *99*, 13368–13379.
(11) Widengren, J.; Dapprich, J.; Rigler, R. *Chem. Phys.* **1997**, *216*, 417–426.
(12) Widengren, J.; Schwille, P. *J. Phys. Chem. A* **2000**, *104*, 6416–6428.
(13) Widengren, J.; Chmyrov, A.; Eggeling, C.; Löfdahl, P.-Å.; Seidel, C. A. M. *J. Phys. Chem. A* **2007**, *111*, 429–440.
(14) Sandén, T.; Persson, G.; Thyberg, P.; Blom, H.; Widengren, J. *Anal. Chem.* **2007**, *79*, 3330–3341.

10.1021/ac1014047
Published on Web 11/24/2010

modulated excitation.[14] Unlike FCS and single-molecule measurements, this so-called transient state (TRAST) monitoring does not require accurate recording of fluorescence time traces, reflecting the spontaneous blinking behavior of individual or a very low number of fluorescent molecules. Likewise, in contrast to single-molecule imaging approaches, where the degree of "blurriness" of the image and its dependence on frame rates or pixel dwell times sometimes can provide information about molecular mobilities,[15,16] the TRAST concept is not restricted to single-molecule concentration samples displaying high molecular fluorescence brightness. It is necessary to modulate the excitation in a predefined manner, but the time information is then entirely kept in the modulation of the excitation. As previously shown,[14] the TRAST concept is therefore fully compatible with low time-resolution detection, for instance by a CCD camera, offering the possibility of a massively parallel readout. The TRAST concept has been realized with time-modulated excitation in a confocal arrangement,[14] in a total internal reflection fluorescence microscope[17] and by use of wide-field imaging.[18] Evidently, the time-modulated excitation experienced by a stationary sample can also be generated by translation of the sample with respect to the excitation, or vice versa. Along this strategy, the TRAST concept was recently established by use of a laser scanning confocal microscope (LSCM).[19]

With the TRAST concept, the response in the time-averaged fluorescence to the modulation characteristics of an excitation pulse train (e.g., duration, height, and separation of the pulses) is used to characterize the population dynamics of photoinduced, long-lived transient states. Vice versa, it is also possible to get information about the modulation characteristics from the same fluorescence response, if the transient state transition properties are known. For a spatially restricted excitation, the effective excitation modulation of the molecules in time is influenced by their passage times through the excitation volume.

On the basis of this notion, we introduce and experimentally verify an approach where the time-averaged fluorescence intensity response from cyanine dye (Cy5) molecules in an open confocal detection volume is used to determine the mobility of the molecules. The passage times of Cy5 were varied by applying a laminar flow. In FCS measurements, cyanine dyes typically show a prominent buildup of nonfluorescent photoisomerized states.[12] By time-modulated excitation the buildup of these states could be made to strongly correlate to the passage times of the molecules through the confocal detection volume, providing a measure of the molecular mobility. The approach was also tested and verified for the fluorescent protein dsRed, where the extent of buildup of a prominent photoinduced transient state of the protein[20] was used to monitor its diffusion speed.

THEORY

Electronic State Model. Most cyanine dyes in their ground states adopt an all-trans conformation.[21] Upon excitation, however, they tend to undergo trans−cis isomerization, whereby one of the double bonds in their polymethine chains undergoes a π-twist around the bond axis (Figure 1A). These formed cis isomers have different absorption spectra and are typically practically nonfluorescent. The isomerization reactions are predominantly light-induced in both directions and occur from one of the excited singlet states of the isomers, N_1 and P_1, to the ground singlet state of the other isomer, P_0 and N_0, respectively. The rates of isomerization from N_1 to P_0 and from P_1 to N_0 are denoted k_{ISO} and k_{BISO}, respectively (caption, Figure 1A). In the absence of excitation, back-isomerization can also occur at room temperature in moderately viscous solvents (k_{PN} in Figure 1A). k_{PN} is on the order of microseconds to milliseconds for most cyanine dyes.[22−24] For the dye Cy5 in aqueous solution it has been found to be on the order of 100 μs or slower.[12]

Given the difference in absorption spectra between the isomers, and that their exchange rates are predominantly light-driven, the steady-state populations of the two isomers relative to each other depend on the excitation wavelength. For Cy5 under excitation with 594, 633, or 647 nm wavelength the fraction of isomers in the trans and cis states are both about 50%.[12]

The quantum yield of intersystem crossing of cyanine dyes is typically quite low, on the order of 10^{-3}.[21,25] Moreover, the lowest triplet state is believed not to be involved in the isomerization process, which has been reported to occur entirely via the excited singlet state.[21,22,26] Singlet−triplet state transitions are therefore not considered in the model of Figure 1A.

In FCS measurements, as well as in the measurements performed in this study, the fluorescence is collected in a confocal manner. For cyanine dyes, the detected fluorescence intensity can be assumed to be proportional to the population of the first excited state N_1 of the trans isomer:

$$F(t) = \int \mathrm{CEF}(\vec{r})\, c(\vec{r}, t)\, q k_{10} \Phi_f\, N_1(\vec{r}, t)\, \mathrm{d}V \qquad (1)$$

Here, $\mathrm{CEF}(\vec{r})$ is the collection efficiency function of the confocal microscope setup, determined by the dimensions of the pinhole and the optical properties of the objective, $c(\vec{r}, t)$ denotes the concentration of fluorophores, and q accounts for the detector quantum efficiency and the attenuation of the fluorescence in the passage from the sample volume to the detector areas. k_{10} is the deactivation rate from the excited singlet state, Φ_f denotes the quantum yield of fluorescence, and $N_1(\vec{r}, t)$ is the fraction of the fluorophores in the detection volume that are in their excited singlet states of the trans isomer. In FCS, the correlation function $G(\tau)$ of the detected fluorescence intensity fluctuations can be considered as a probability distribution of detecting a photon from a fluorescent molecule at time τ, given

(15) Elf, J.; Li, G.-W.; Xie, X. S. *Science* **2007**, *316*, 1191–1194.
(16) Vukojević, V.; Heidkamp, M.; Ming, Y.; Johansson, B.; Terenius, L.; Rigler, R. *Proc. Natl. Acad. Sci. U.S.A.* **2008**, *105*, 18176–18181.
(17) Spielmann, T.; Blom, H.; Geissbühler, M.; Lasser, T.; Widengren, J. *J. Phys. Chem. B* **2010**, *114*, 4035–4046.
(18) Geissbühler, M.; Spielmann, T.; Formey, A.; Märki, I.; Leutenegger, M.; Hinz, B.; Johnsson, K.; Van De Ville, D.; Lasser, T. *Biophys. J.* **2010**, *98*, 339–349.
(19) Sandén, T.; Persson, G.; Widengren, J. *Anal. Chem.* **2008**, *80*, 9589–9596.
(20) Malvezzi-Campeggi, F.; Jahnz, M.; Heinze, K. G.; Dittrich, P.; Schwille, P. *Biophys. J.* **2001**, *81*, 1776–1785.
(21) Aramendia, P. F.; Negri, R. M.; Roman, E. S. *J. Phys. Chem.* **1994**, *98*, 3165–3173.
(22) Kuzmin, V. A.; Darmanyan, A. P. *Chem. Phys. Lett.* **1978**, *54*, 159–163.
(23) Sundström, V.; Gillbro, T. *J. Phys. Chem.* **1982**, *86*, 1788–1794.
(24) Chibisov, A. K.; Zakharova, G. V.; Görner, H. *J. Chem. Soc., Faraday Trans.* **1996**, *92*, 4917–4925.
(25) Krieg, M.; Redmond, R. W. *Photochem. Photobiol.* **1993**, *57*, 472–479.
(26) Chibisov, A. K. *J. Photochem.* **1977**, *6*, 199–214.

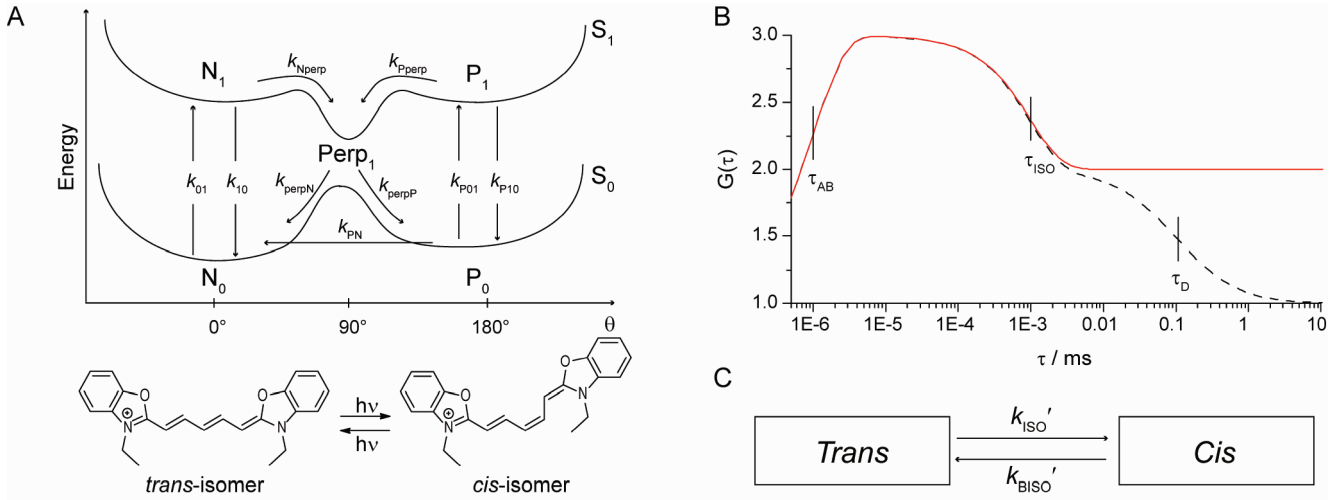

Figure 1. (A) Kinetic scheme modeling the photophysical behavior of carbocyanine dyes. N_0 and N_1 denote the ground singlet and the first excited singlet states of the thermodynamically stable conformation of the dye, normally the all-trans form (bottom left). P_0 and P_1 are the corresponding states of the photoisomerized form, usually a monocis conformation (bottom right). Upon isomerization the angle, θ, in one of the double bonds of the conjugated hydrocarbon chain connecting the two headgroups of the dye is twisted by 180°. Transitions from N_1 and P_1 take place via the partially twisted intermediate state, $Perp_1$, either to N_0 or to P_0. $k_{01} = \sigma_{01} I_{EXC}$ denotes the excitation rate from N_0 to N_1 (where σ_{01} is the excitation cross section of N_0 and I_{EXC} is the excitation irradiance). $k_{P01} = \sigma_{P01} I_{EXC}$ is the corresponding excitation rate from P_0 to P_1. k_{PN} is the rate of thermal deactivation of P_0 to N_0. The isomerization rates from P_1 to N_0 and from N_1 to P_0 can be expressed as $k_{ISO} = k_{Pperp}[k_{perpN}/(k_{perpN} + k_{perpP})]$ and $k_{BISO} = k_{Nperp}[k_{perpP}/(k_{perpN} + k_{perpP})]$, respectively. (B) Calculated FCS curve (dotted) and the corresponding population of the excited singlet state N_1 for Cy5 vs τ (red), given the initial population probabilities at $\tau = 0$ of $N_1 = 1$, $N_0 = 0$, $P_1 = 0$, $P_0 = 0$. Fluorescence antibunching time $\tau_{AB} = 10^{-9}$ s, isomerization relaxation time $\tau_{ISO} = 10^{-6}$ s, and characteristic diffusion time $\tau_D = 10^{-3}$ s. (C) Two-state model used to characterize the isomerization-induced fluorescence fluctuations observed in the FCS experiments. Here Trans and Cis correspond to the fractions of dye molecules in the detection volume that are in their trans singlet ($N_0 + N_1$) and cis singlet ($P_0 + P_1$) states. k_{ISO}' and k_{BISO}' denote the effective rates of isomerization and back-isomerization (eqs 3 and 4).

that a photon was detected from the same molecule at time 0. A typical FCS curve for a cyanine dye, measured in aqueous solution and undergoing trans−cis isomerization upon excitation, is shown in Figure 1B, and can be expressed as[12]

$$G_{ISO}(\tau) = \frac{1}{N}\left[1 + \frac{\tau}{\tau_D}\right]^{-1}\left[1 + \left(\frac{\omega_0}{\omega_z}\right)^2 \frac{\tau}{\tau_D}\right]^{-1/2} \times \left[1 + \frac{P_{eq}}{1 - P_{eq}} \exp(-\tau/\tau_{ISO})\right] \quad (2)$$

Here, N is the mean number of fluorescent molecules within the detection volume. ω_0 and ω_z are the distances from the center of the laser beam focus in the radial and axial direction, respectively, at which the collected fluorescence intensity has dropped by a factor of e^2 compared to its peak value. The characteristic diffusion time for the fluorescent molecules is given via the diffusion coefficient, D, by $\tau_D = \omega_0^2/4D$. P_{eq} is the time- and space-averaged fraction of fluorophores within the detection volume being in a nonfluorescent cis photoisomer form, and τ_{ISO} is the relaxation time related to the trans−cis isomerization process.

Considering that equilibration between the ground and excited singlet states within both the isomers (approximately nanoseconds) has already occurred at the time scale of the isomerization (approximately microseconds to milliseconds), the electronic state model of Figure 1A can be simplified to a two-state model (Figure 1C). In this model, it is further assumed that triplet state formation can be neglected. The effective rates of isomerization and back-isomerization can then be expressed as

$$k_{ISO}' = \frac{k_{01}}{k_{10} + k_{01}} k_{ISO} = \frac{\sigma_{01} I_{EXC}}{k_{10} + \sigma_{01} I_{EXC}} k_{ISO} \quad (3)$$

$$k_{BISO}' = \frac{k_{P01}}{k_{P10} + k_{P01}} k_{BISO} + k_{PN} = \frac{\sigma_{P01} I_{EXC}}{k_{P10} + \sigma_{P01} I_{EXC}} k_{BISO} + k_{PN}$$
$$\{k_{P10} \gg \sigma_{P01} I_{EXC}\} = \sigma_{BISO} I_{EXC} + k_{PN} \quad (4)$$

Here σ_{01} and σ_{P01} are the excitation cross sections of the ground singlet states N_0 and P_0, respectively. I_{EXC} denotes the mean excitation irradiance within the detection volume. k_{10} and k_{P10} are the deactivation rates of the singlet excited states N_1 and P_1, respectively. Approximating the excitation irradiance within the detection volume to be uniform,[12,14] P_{eq} and τ_{ISO} of eq 2 can then be expressed as

$$P_{eq} = \frac{k_{ISO}'}{k_{ISO}' + k_{BISO}'} \quad (5)$$

$$\tau_{ISO} = (k_{ISO}' + k_{BISO}')^{-1} \quad (6)$$

MATERIALS AND METHODS

Instrumental Setup. A home-built confocal setup, consisting of an Olympus IX-70 microscope body with a 60×, NA 1.2, UPlanApo Olympus objective was used for the measurements. For measurements with Cy5, excitation was done by a linearly polarized He−Ne laser (594 nm, Laser2000 model 30572, Munich, Germany), attenuated by neutral density filters (Schott, Germany) down to 150 μW. The laser beam was reflected by a dichroic

mirror (z488/594rpc, Chroma Technology Corp., U.S.A.) and focused down to a $1/e^2$ radius of $\omega_0 = 0.38\ \mu$m (estimated from the diffusion times of Cy5 acquired from FCS measurements with different pinhole sizes). Emitted fluorescence was collected by the same objective and focused by a 150 mm achromatic lens onto a pinhole of 80 μm diameter in the image plane. Direct Rayleigh-scattered light from the laser beam and Raman-scattered light from the aqueous solution were suppressed by use of band-pass filters (HQ675/135M, Chroma Technology Corp., U.S.A.) prior to fluorescence detection by two avalanche photodiodes (APDs) (SPCM AQR-14/16, Perkin-Elmer Optoelectronics, U.S.A.) in a 50/50 beam-splitting arrangement (BS010, Thorlabs, U.S.A.), to eliminate detector afterpulsing and shot noise. Laser intensity modulation was performed by an acousto-optic modulator (AOM; AA.MT.200/A0,5-VIS, AA Opto-Electronic, Orsay, France).

For measurements with the DsRed fluorescent protein, 514 nm excitation was provided by a linearly polarized multiline argon-ion laser (Lasos LGK 7812 ML, Jena, Germany) and an excitation filter (Z514/10×, Chroma Technology Corp., U.S.A.). Laser power was set to 500 μW. The excitation volume was expanded to a $1/e^2$ radius of $\omega_0 = 1.9\ \mu$m (estimated from the diffusion times of rhodamine 6G acquired from FCS measurements with different pinhole sizes). For these measurements a pinhole with diameter 200 μm was used. Dichroic mirror (515/633PC) and fluorescence emission filters (HQ580/80M) were from Chroma Technology Corp., U.S.A.

For both the Cy5 and the dsRed measurements, the residence times of the molecules inside of the excitation volume were controlled by applying different flow rates through a microchannel in a silicone film of 200 μm height and 2 mm width. A syringe pump (SP101i, World Precision Instruments Inc., U.S.A.) was used to regulate the flow rates.

Data Collection and Processing. The procedures for the data collection and processing were largely based on those developed in refs 14 and 19. Data were collected using a PCI-6602 counter/timer card (National Instruments Corp., U.S.A.), counting pulses from two APDs connected to separate channels (counters). The acousto-optical modulator driver was externally controlled by a digital signal generated by the card. Communication with the data collecting card PCI-6602 was done via a dynamic-link library (DLL) driver written in C with use of an application programming interface (API) NI-DAQmx. Measurements were automated by Matlab (The MathWorks, Inc., U.S.A.) based software developed in house. With this software, series of excitation pulse trains could be generated, for which the period time, T, and the excitation pulse width, w, could be changed in an automated, preprogrammed manner from one pulse train to the next. The internal 80 MHz clock of the card was used as a time base for the modulation.

For each modulation setting (i.e., for each excitation pulse train with a defined T and w) the fluorescence was recorded and averaged over the full duration of the pulse train (2 s for Cy5 measurements, 15 s for DsRed measurements). After each pulse train, excitation and acquisition were turned off for 0.1 s, to allow for full electronic-state relaxation within the fluorophore molecules before the onset of the next pulse train.

The software generated a matrix with the time-averaged fluorescence intensities, $\bar{F}$, for each pulse train, with period time, T, and pulse width, w. Before measurement on a sample, an intensity matrix was acquired for a blank, i.e., buffer solution in an identical sample container. This background matrix was then directly subtracted from the intensities measured for the samples by the software. $\bar{F}$ were also corrected for possible nonlinear responses of the detectors, appearing at fluorescence interphoton times approaching those of the dead time of the APDs.

The measured average fluorescence intensities, $\bar{F}$, were divided with the modulation duty cycles, η, of their corresponding excitation pulse trains. Thereby, the average fluorescence intensity during the time the excitation light was actually on, i.e., $\bar{F}_{EXC}$ of eq 16, could be calculated.

For the FCS measurements, the APD signals from each detection channel were processed by an ALV-5000/E correlator (ALV-GmbH, Germany), with an ALV 5000/FAST tau extension board giving a 12.5 ns lag time resolution when cross-correlating between channels.

Sample Preparation. Cy5 monomaleimide was purchased from GE Healthcare (U.K.), dissolved in DMSO, and subsequently diluted to nanomolar concentrations in ultrafiltered, distilled water (Easypure, Wilhelm Werner GmbH, Germany). DsRed fluorescent protein was a kind gift from Professor Masataka Kinjo, Hokkaido University, Japan. The protein was diluted to nanomolar concentrations in Dulbecco's phosphate-buffered saline pH 7.4 (Sigma-Aldrich, U.S.A.)

RESULTS AND DISCUSSION

Concept of Measurements. As shown recently,[14,19] the dependence of the time-averaged fluorescence on the modulation characteristics of the excitation (e.g., duration, height, and separation of the pulses within an excitation pulse train) can be used to extract information about the population dynamics of photoinduced, long-lived transient states of dyes. Vice versa, if the transient state transition properties of the dye are known it is also possible to get information about the modulation characteristics from the fluorescence response. For a spatially restricted excitation, the effective excitation modulation of the molecules over time can also be influenced by their passage times through the excitation volume. On the basis of known transient dark state characteristics of the fluorescent molecules, the laser excitation modulation can be adapted so that the response in the average fluorescence is particularly sensitive to the dwell times of the fluorescent molecules in the excitation volume. This concept to determine molecular dwell times or diffusion properties can in principle be realized, utilizing the kinetic properties of a range of transient photoinduced states. However, trans−cis isomerization offers an additional advantage, in that it is light-driven in both directions. Apart from a slow thermal deactivation by k_{PN} the two isomers do not interconvert in the absence of excitation. The extent of buildup of cis isomers thus reflects the amount of excitation irradiation that the molecules have been exposed to. In other words, for a known excitation irradiance, it reflects how much time the molecules on average have spent in the excitation volume. By modulation, the distribution of the excitation irradiation in time can be adapted so that the extent of buildup of the transient state, in our case the cis isomer, is maximally sensitive to changes in the dwell times of the

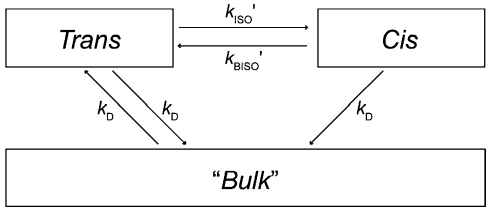

Figure 2. Three-state model used to characterize the fluorescence intensities observed in the modulated excitation experiments. Here, the states "Trans" and "Cis" and the rates k_{ISO}' and k_{BISO}' are defined as in Figure 1C. The "Bulk" state represents the molecules outside of the excitation volume, and k_D is the rate of exchange of molecules into and out of this volume.

molecules in the excitation volume. For this purpose, we introduced a square-wave modulation of the excitation in time, with the excitation irradiance within each pulse period given by

$$I_{EXC}(t) = \begin{cases} I_{EXC}, & 0 < t \le w \\ 0, & w < t \le T \end{cases} \tag{7}$$

Here, T is the period time, w is the duration of the excitation pulse within each period, and I_{EXC} is the excitation irradiance. In the following, we use a time variable t, which is reset to $t = 0$ after each pulse period. For the first excitation pulse, assuming uniform excitation irradiance within the detection volume and the molecules to be immobile, the time development of the fluorescence intensity at onset of excitation follows that of the excited singlet state of the trans isomer and is analogous to the relaxation displayed in the FCS curves (eq 2):

$$F(t) \propto N_1(t) \propto 1 - P_{eq} + P_{eq} \exp(-\tau/\tau_{ISO}) \tag{8}$$

To take diffusion into and out of the detection volume into account, the diffusional exchange is approximated as a chemical reaction interconverting "in volume" and "bulk" molecules with an effective rate k_D in both directions. Thereby, the dwell times of the fluorophores in the volume are approximated to be exponentially distributed.

A modified kinetic scheme based on this approximation is presented in Figure 2. From this scheme, a set of coupled first-order differential equations can be established:

$$\frac{d}{dt}\begin{pmatrix} \mathrm{Trans}(t) \\ \mathrm{Cis}(t) \\ \mathrm{Bulk}(t) \end{pmatrix} = \begin{bmatrix} -k_{ISO}' - k_D & k_{BISO}' & k_D \\ k_{ISO}' & -k_{BISO}' - k_D & 0 \\ k_D & k_D & -k_D \end{bmatrix} \begin{pmatrix} \mathrm{Trans}(t) \\ \mathrm{Cis}(t) \\ \mathrm{Bulk}(t) \end{pmatrix} \tag{9}$$

where k_{ISO}' and k_{BISO}' are the effective rates of isomerization and back-isomerization, as defined in eqs 3 and 4, and k_D denotes the rate of exchange of molecules into and out of the excitation volume (Figure 2).

"Trans" and "Cis" denote the normalized populations of the trans (in either N_0, or N_1) and cis (in either P_0 or P_1) isomers, respectively. "Bulk" is the population of the fluorophores in the solution outside of the detection volume. The concentration of fluorescent molecules is assumed to be constant and normalized to unity both inside and outside of the detection volume:

$$\begin{aligned} \mathrm{Trans}(t) + \mathrm{Cis}(t) &= 1 \\ \mathrm{Bulk}(t) &= 1 \end{aligned} \tag{10}$$

At onset of the first excitation pulse of the pulse train, the following initial condition is valid:

$$\begin{pmatrix} \mathrm{Trans}_0^{off}(T) \\ \mathrm{Cis}_0^{off}(T) \\ \mathrm{Bulk}_0^{off}(T) \end{pmatrix} = \begin{pmatrix} \mathrm{Trans}_1^{on}(0) \\ \mathrm{Cis}_1^{on}(0) \\ \mathrm{Bulk}_1^{on}(0) \end{pmatrix} = \begin{pmatrix} 1 \\ 0 \\ 1 \end{pmatrix} \tag{11}$$

Here, X_i^p signify the population probability of state X (= Trans, Cis, or Bulk), with the superscript p (= on or off) denoting whether the excitation is active or idle and the subscript i denoting the number of the pulse within the pulse train.

From the initial condition of eq 11 and the set of differential equations of eq 9, the population dynamics of the trans and cis state within the excitation pulse ($0 < t \le w$) can be described by

$$\begin{aligned} \mathrm{Trans}_i^{on}(t) &= 1 - \frac{k_{ISO}'}{k_\Sigma} + \exp(-tk_\Sigma)\left[-\mathrm{Cis}_{i-1}^{off}(T) + \frac{k_{ISO}'}{k_\Sigma}\right] \\ \mathrm{Cis}_i^{on}(t) &= \frac{k_{ISO}'}{k_\Sigma} + \exp(-tk_\Sigma)\left[\mathrm{Cis}_{i-1}^{off}(T) - \frac{k_{ISO}'}{k_\Sigma}\right] \end{aligned} \tag{12}$$

Here $k_\Sigma = k_{ISO}' + k_{BISO}' + k_D$.

When the excitation is turned off, k_{ISO}' is 0, and the population time development within the time period between two consecutive pulses ($w < t \le T$) is given by

$$\begin{aligned} \mathrm{Trans}_i^{off}(t) &= 1 - \mathrm{Cis}_i^{on}(w)\exp(-[t-w][k_D + k_{PN}]) \\ \mathrm{Cis}_i^{off}(t) &= \mathrm{Cis}_i^{on}(w)\exp(-[t-w][k_D + k_{PN}]) \end{aligned} \tag{13}$$

Applying the initial condition of eq 11, at the start of the excitation pulse train, and then using eqs 12 and 13 recursively for $i = 1, 2, 3, \ldots, n$, the population dynamics can be calculated for a square-wave pulse train of n pulse periods, as described by eq 7.

Equilibration between the ground and first excited singlet states occur on the nanosecond time scale, which is much shorter than the typical pulse widths applied (several microseconds). Consequently, within the ith excitation pulse ($0 < t \le w$):

$$N_{1,i}(\vec{r}, t) = \frac{\sigma_{01} I_{EXC}}{k_{01} + \sigma_{01} I_{EXC}} \mathrm{Trans}_i^{on}(\vec{r}, t) \tag{14}$$

When the excitation pulse is ended, N_1 decays within nanoseconds to N_0. In between the excitation pulses ($w < t \le T$), the population of N_1 can thus be set to zero.

For a measurement with n excitation pulses, the average fluorescence signal during the measurement is then given by

$$\bar{F} = \frac{1}{nT}\int_0^{nT} F(t)\,dt = Q\frac{1}{nT}\sum_{i=1}^{n}\left[\int_0^w N_{1,i}(t)\,dt\right] \tag{15}$$

Here nT is the total duration of the excitation pulse train and Q is the product of the constants q, k_{10}, and Φ_f from eq 1 and the integral $\int CEF(\vec{r})c(\vec{r}, t)\,dV$, which is assumed to remain constant (no photobleaching).

Dividing the average detected fluorescence with the pulse train duty cycle ($\eta = w/T$) yields the average fluorescence intensity within the excitation pulses:

$$\bar{F}_{EXC} = \bar{F}/\eta \tag{16}$$

Experimental Verification. The concept was experimentally tested by measurements of freely diffusing Cy5 in aqueous solution. FCS measurements (Supporting Information Figure S-3) were performed at different excitation irradiancies (from 10 to 300 kW/cm^2) to determine the rates of photoinduced isomerization and back-isomerization and to check the diffusion properties of the dye. By fitting the FCS curves to eq 2, the diffusion coefficient of Cy5 was determined to $D = 3.9 \times 10^{10}$ m^2/s (at 22 °C). From the excitation dependence of τ_{ISO} and P_{eq}, obtained by fitting the FCS curves to eq 2 and then using eqs 3−6, yielded $k_{ISO} = 23\ \mu s^{-1}$ and $\sigma_{BISO} = 0.03 \times 10^{-16}$ cm^2. Here, σ_{01} was set to 1.3×10^{-16} cm^2 and k_{10} to 1160 μs^{-1}.[12] The values of k_{ISO} and σ_{BISO}, as well as the diffusion coefficient, D, of Cy5 are well in agreement with previously determined parameter values using FCS[12] and dual-foci FCS.[27] On the basis of the determined isomerization parameters, the behavior of the box model of Figure 2 was tested by calculating the time dependence of the fluorescence and population levels of the trans and cis isomers for square-wave excitation pulse trains with different pulse characteristics. Further, pulse characteristics were identified yielding a clear distinction in the measured $\bar{F}_{EXC}$ for immobile molecules and molecules freely diffusing into and out of the excitation volume (see the Supporting Information).

On the basis of these pulse characteristics, excitation-modulated measurements on fluorescent molecules were performed with different excitation volume residence times. Different residence times can be achieved by coupling the Cy5 fluorophore molecule to molecules of different sizes. However, a more convenient and tunable approach is to vary the residence times of the fluorophores by applying different flow speeds in a microchannel. The flow speeds were analyzed with FCS (Supporting Information Figure S-4) using the following expression:[28,29]

$$G(\tau) = G_{ISO}(\tau) \exp\left(-\left[\frac{\tau}{\tau_{flow}}\right]^2\left[1 + \frac{\tau}{\tau_D}\right]^{-1}\right) \tag{17}$$

where $G_{ISO}(\tau)$ is defined by eq 2. τ_{flow} is the average (laminar) flow time of the fluorescent molecules through the detection volume, from which the flow velocity is given by $V = \tau_{flow}/\omega_0$. V was found to depend linearly on the applied flow rates of aqueous solution through the microchannel (inset of Supporting Information Figure S-4).

At low flow rates (few microliters/min), the characteristic flow times τ_{flow}, as obtained from the FCS measurements, are lower than the diffusion time τ_D. τ_{flow} is then not representative for the molecular residence times. As a more general estimate of the residence times at different flow rates, providing also a relation between the measured k_D and the molecular diffusion properties, one may use the integral of the area of the correlation curve representing diffusion and/or flow:

$$\tau_{residence} = \int_0^\infty G_D(\tau) G_{flow}(\tau)\, d\tau \tag{18}$$

where

$$G_D(\tau) = \left(1 + \frac{\tau}{\tau_D}\right)^{-1}\left(1 + \frac{\tau}{(z_0/\omega_0)^2\tau_D}\right)^{-1/2}$$

and

$$G_{flow}(\tau) = \exp\left(-\left[\frac{\tau}{\tau_{flow}}\right]^2\left[1 + \frac{\tau}{\tau_D}\right]^{-1}\right)$$

with

$$\tau_D = \omega_0^{\,2}/4D$$

By applying different flow rates in the microchannel, $\tau_{residence}$ was varied from 130 to ~40 μs, as measured by FCS in the same setup, but without excitation modulation, before and after each series of the excitation-modulated measurements. For each adjusted flow rate, $\bar{F}_{EXC}$ was measured under excitation modulation, varying the pulse widths, w (1−5 μs), and the pulse periods, T (5−300 μs) of the different pulse trains. A significant increase in $\bar{F}_{EXC}$ could be observed with increasing T, for pulse widths shorter than the residence times of the fluorophores (Figure 3A). The duration of each pulse train was 2 s. The power of the pulses was kept constant for all pulse trains and corresponded to an average excitation irradiance of 34 kW/cm^2 in the detection volume.

The measured $\bar{F}_{EXC}$ and its variation with T and w were analyzed by the model of Figure 2.

The acquired $\bar{F}_{EXC}$ data were fitted to eqs 15 and 16. In the fitting, σ_{01} and σ_{BISO} were fixed to 1.3×10^{-16} cm^2 and 0.03×10^{-16} cm^2, respectively,[12] k_{10} to 1.16×10^9 s^{-1}, k_{ISO} to 25×10^6 s^{-1}, and k_{PN} to 1×10^4 s^{-1}. Only the diffusion rate (k_D) was entered as a free parameter. In Figure 3B, the resulting inverse diffusion rates, $1/k_D$, are plotted versus $\tau_{residence}$, as determined from the corresponding FCS. This plot yields a close to linear relationship between $1/k_D$ and $\tau_{residence}$, as predicted from the model of Figure 2. Repeating the measurements under the same conditions, this linear relationship and its slope was reproduced within 10% (data not shown). The simplified model of Figure 2 reflects molecular exchange due to flow more accurately than due to diffusion, but relative changes should be detectable and can be related to the diffusion behavior by eq 18. For high flow rates, the flow speeds can be approximated from k_D by $V = 2\omega_0 k_D$ and were found to agree well with the flow speeds determined from the FCS measurements (Supporting Information Figure S-4).

To test how the estimation of the photophysical parameters in the model may affect the determined k_D above, fits to the data in Figure 3A were performed where the parameter values of σ_{01}, σ_{BISO}, k_{10}, and k_{PN} were fixed as stated above, except that one of the parameters was set to different values, by −50% up to +50% off the correctly fixed value. Variation of the fixed parameter values of σ_{exc}, σ_{BISO}, k_{10} one by one then resulted in

(27) Loman, A.; Dertinger, T.; Köberling, F.; Enderlein, J. *Chem. Phys. Lett.* **2008**, *459*, 18–21.
(28) Magde, D.; Webb, W. W.; Elson, E. L. *Biopolymers* **1978**, *17*, 361–376.
(29) Gösch, M.; Blom, H.; Holm, J.; Heino, T.; Rigler, R. *Anal. Chem.* **2000**, *72*, 3260–3265.

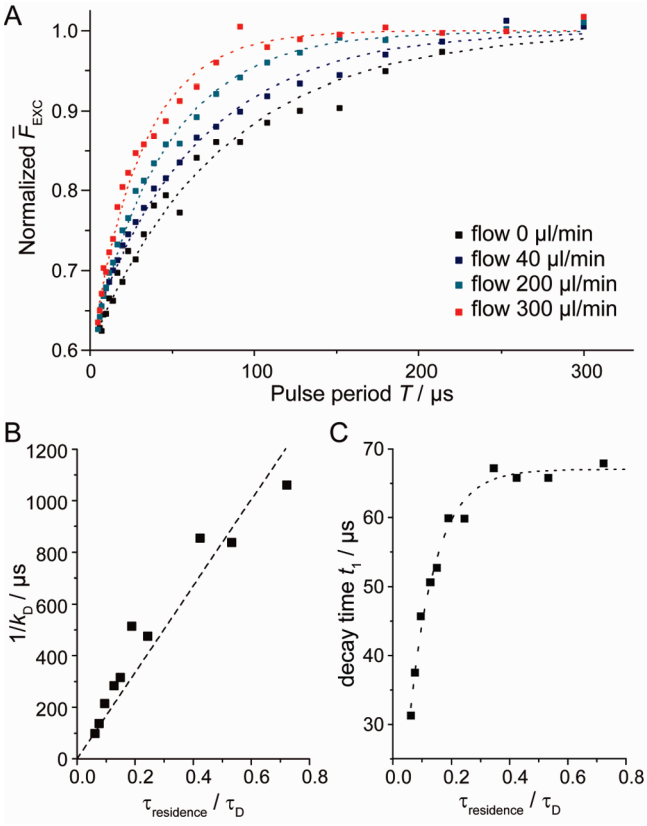

Figure 3. (A) Measured average fluorescence intensity within the excitation pulses, $\bar{F}_{exc}$, for Cy5 with different flow rates 0−300 μL/min. For all measurements, the pulse width $w = 2.0$ μs and the pulse period T was varied from 5.1 to 300 μs. $\bar{F}_{exc}$ is normalized to 1 for the longest $T = 300$ μs. Excitation irradiance was 34 kW/cm^2. The measurement time was 2 s for each data point. Dotted lines: fit according to eq 15. (B) Inverse of the diffusion rate k_D obtained by fitting the data in plot A to eq 15. On the abscissa: the normalized residence time ($\tau_{residence}/\tau_D$) calculated according to eq 18. A linear dependence of $1/k_d$ vs $\tau_{residence}$ could be observed. (C) The inverse of the single-exponential decay time t_1 obtained as a result of fitting the data in plot A to eq 19. The dependence of t_1 vs the normalized residence time follows an inverse single-exponential decay, given by $t_1 = t_{PN}[1 - \exp[(\tau_{residence}/\tau_D)/\tau_{PN}]]$, yielding the parameter values $t_{PN} = 68$ μs and $\tau_{PN} = 0.09$. measurements.

comparable relative errors in the determined k_D values. By variation of the fixed k_{PN} value, however, severalfold larger deviations in the determined k_D values were found. This strong dependence of k_D on the fixed k_{PN} value reflects that the analysis relies on a strong correlation between the excitation irradiation dose and the dark state buildup, which in turn depends on the extent to which the transitions to and from the dark state are light-induced, i.e., on the value of k_{PN}.

To test the possible influence of photobleaching in the measurements, finite element method (FEM) simulations were performed assuming a Gaussian−Lorentzian shaped excitation volume with the same dimensions and excitation conditions as in the experiments, and assuming an irreversible photobleaching rate $k_B(\bar{r}, t) = \Phi_B k_{10} N_1(\bar{r}, t)$, where Φ_B denotes the photobleaching quantum yield (2×10^{-5} for Cy5[12]). For the worst case (no flow and at the highest excitation duty cycles (shortest T)) the average concentration depletion of Cy5 in the detection volume reaches 3%. In relation to the amplitudes of the recovery curves in Figure 3A this is a minor effect, which is also mainly restricted to the data points recorded under no flow and at high excitation duty cycles.

Apart from the analysis based on this model, we noted that the normalized fluorescence $\bar{F}_{EXC}$, plotted versus the pulse period T (Figure 3A) could also be well-fitted to a negative single-exponential function:

$$y(t) = y_0 - A \exp(-t/t_1) \tag{19}$$

where the parameters y_0 and A were found to be relatively constant for the different flow rates ($y_0 \sim 2050$ kHz and $A \sim 800$), and where t_1 initially increases with increasing $\tau_{residence}$ and then reaches an asymptotic value (Figure 3C). We assume that this asymptotic value of t_1 reflects the isomerization relaxation time, given by the thermal back-isomerization of the dyes, $1/k_{PN}$, which then also defines a lower limit for how slow molecular transits that can be monitored via this particular photophysical process.

A range of fluorescent proteins display long-lived non- or weakly emitting states with photodynamic features very similar to trans−cis isomerization of cyanine dyes.[30−33] For this reason, excitation-modulated measurements were also performed in the same manner on the fluorescent protein DsRed. In agreement with previous observations,[20] FCS measurements of DsRed in aqueous solution revealed a prominent dark state relaxation component, with relative amplitude of about 30% and with a relaxation time in the submillisecond time range. As for trans−cis isomerization of Cy5, the amplitude of the relaxation component remained constant (except for a minor drop for lower I_{EXC}, possibly attributed to a larger relative influence of thermal back-isomerization), while the relaxation time decreased with higher excitation intensities (Supporting Information Figure S-5). Given the relatively slow isomerization dynamics of dsRed, the excitation volume was enlarged, yielding diffusion times of DsRed of ~15 ms, as measured by FCS. The isomerization dynamics in DsRed is significantly more complex than in Cy5. As for many fluorescent proteins a multitude of photoinduced states can be expected, with relaxation times found over a broad time range. We therefore did not apply the model described by eqs 15 and 16 to evaluate the DsRed measurements. However, as in the Cy5 measurements the normalized fluorescence $\bar{F}_{EXC}$ versus the pulse train period was found to fit well to eq 19 (Figure 4). Moreover, as for Cy5, the t_1 parameter values obtained from these fits displayed a negative exponential dependence to $\tau_{residence}$, (inset of Figure 4). Consequently, although the complex photophysics of DsRed at least at a first attempt excludes an evaluation using the model of Figure 2, the recovery curves of Figure 4 support the applicability of the proposed method for protein mobility studies using also fluorescent proteins.

(30) Haupts, U.; Maiti, S.; Schwille, P.; Webb, W. W. *Proc. Natl. Acad. Sci. U.S.A.* **1998**, *95*, 13573–13578.
(31) Widengren, J.; Mets, Ü.; Rigler, R. *Chem. Phys.* **1999**, *250*, 171–186.
(32) Jung, G.; Wiehler, J.; Zumbusch, A. *Biophys. J.* **2005**, *88*, 1932–1947.
(33) Blum, C.; Subramaniam, V. *Anal. Bioanal. Chem.* **2009**, *393*, 527–541.

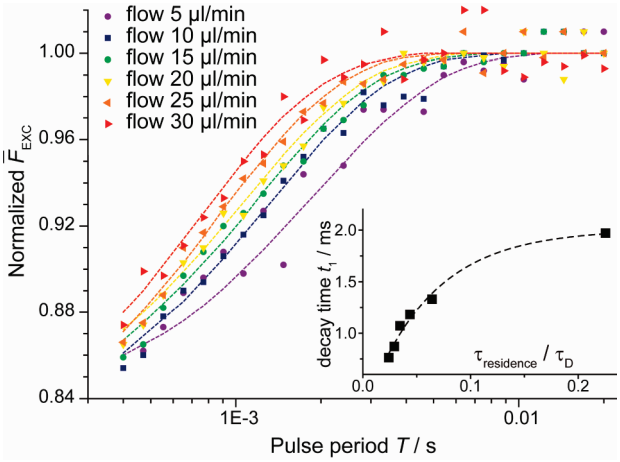

Figure 4. $\bar{F}_{exc}$ obtained from time-modulated excitation measurements on DsRed applying different flow rates (5−30 μL/min). For all measurements, w = 300 μs and T was varied from 0.4 to 20 ms. Curves are normalized to 1 for the longest T = 20 ms. The excitation irradiance was 4.4 kW/cm^2. Measurement times: 15 s for each data point. Dotted lines: single-exponential fit according to eq 19. Inset: the t_1 parameter values obtained from fitting $\bar{F}_{exc}$ vs T to eq 19, plotted vs the residence time, calculated according to eq 18. Parameter values obtained from an inverse exponential fit, as in Figure 3C: t_{PN} = 1.9 ms and τ_{PN} = 0.06.

As for the Cy5 measurements, the influence of photobleaching in the dsRed measurements of Figure 4 was investigated by FEM simulations, using a $\Phi_B = 8 \times 10^{-6}$.[34−36] For the worst case (flow rate 5 μL/min, T = 0.4 ms), we estimate an average concentration depletion in the excitation volume of up to 6%. However, with exception of the first three data points with flow 5 μL/min (T < 0.6 ms) and the first data point with flow 10 μL/min (T = 0.4 ms) the photobleaching depletion for the remaining 146 data points is well below 3%. The recovery curves in Figure 4 can therefore almost fully be attributed to the recovery from the transient dark state of dsRed. Moreover, in this study, the excitation intensities were set relatively high to allow comparative measurements with FCS (Supporting Information). In general, by applying lower excitation intensities, the effects of photobleaching will be further diminished.

CONCLUDING REMARKS

In this work, we demonstrate a concept where the mobilities of fluorescent molecules into and out of a spatially restricted excitation volume, and subject to properly adapted time-modulated excitation in this volume, can strongly influence the buildup of nonfluorescent transient states in the fluorophores. This transient state buildup is in turn reflected in the detected time-averaged fluorescence intensity, which can be used to characterize the mobilities of the molecules.

By the concept, diffusion measurements can be performed in the same spatial and temporal range as that of FCS, and in contrast to FRAP it exploits a mechanism that does not irreversibly deplete the sample fluorescence. In contrast to FCS measurements, it can be performed with very small constraints in the concentration range and with practically no need for a high fluorescence brightness of the molecules studied. Here, molecular mobility measurements were demonstrated for fluorophores traversing a single focused laser beam. However, since the concept can be performed with very minor requirements in terms of time resolution and sensitivity in the detection, also a more parallelized approach should be possible. Such readout can be realized by introducing a patterned or wide-field excitation, modulated in time and/or space, and by using a standard CCD camera for fluorescence detection. For the Cy5 measurements in this study, the relevant photophysical parameters were known and the fluorescence data was fitted with the k_D rate as the only free parameter. However, in general the photophysical parameters can be rather environmentally sensitive and for more complex environments not always easily determined. Our parameter stability tests show that in particular the thermal deactivation rate of the dark cis state (k_{PN}) is critical and sets a lower limit for how slow transits that can be monitored. Nonetheless, when measuring under similar environmental conditions the proposed approach should be able to provide relative mobility information, as illustrated by the dsRed measurements. Moreover, if the k_{PN} rate of Cy5 would not be small enough to monitor slowly moving molecules, dsRed or other fluorophores or fluorescent proteins[37] can be used having considerably smaller thermal deactivation rates. With these aspects in mind, we expect the proposed method to be useful for biomolecular mobility imaging, in cells or in vitro, where the mobility of the molecules is too fast to be recorded within the frame rates of commonly used microscopic techniques, such as laser-scanning confocal microscopy and wide-field or total-internal reflection microscopy using a CCD camera for fluorescence detection. It may also provide a complement to FCS and FRAP for localized molecular mobility studies, where instrumental constraints or the concentration range and/or the molecular fluorescence brightness of the sample may pose limitations.

(34) Baird, G. S.; Zacharias, D. A.; Tsien, R. Y. *Proc. Natl. Acad. Sci. U.S.A.* **2000**, *97*, 11984–11989.
(35) Heikal, A. A.; Hess, S. T.; Baird, G. S.; Tsien, R. Y.; Webb, W. W. *Proc. Natl. Acad. Sci. U.S.A.* **2000**, *97*, 11996–12001.
(36) Lounis, B.; Deich, J.; Rosell, F. I.; Boxer, S. G.; Moerner, W. E. *J. Phys. Chem. B* **2001**, *105*, 5048–5054.
(37) Fuchs, J.; Bohme, S.; Oswald, F.; Hedde, P. N.; Krause, M.; Wiedenmann, J.; Nienhaus, G. U. *Nat. Methods* **2010**, *7*, 627–U35.

ACKNOWLEDGMENT

This study was supported by funding from the European Community's Seventh Framework Programme (FLUODIAMON, 201 837), the Swedish Research Council, and the Knut and Alice Wallenberg Foundation.

SUPPORTING INFORMATION AVAILABLE

Additional information as noted in text. This material is available free of charge via the Internet at http://pubs.acs.org.

Received for review May 28, 2010. Accepted November 4, 2010.

AC1014047